Plasticization, Antiplasticization, and Molecular Packing in Amorphous Carbohydrate−Glycerol Matrices

ARTICLE *in* BIOMACROMOLECULES · NOVEMBER 2010

Impact Factor: 5.75 · DOI: 10.1021/bm1005068 · Source: PubMed

4 AUTHORS, INCLUDING:

Mina Roussenova
University of Bristol
15 PUBLICATIONS **209** CITATIONS
SEE PROFILE

Mathieu Murith
Nestlé S.A.
3 PUBLICATIONS **50** CITATIONS
SEE PROFILE

Plasticization, Antiplasticization, and Molecular Packing in Amorphous Carbohydrate-Glycerol Matrices

Mina Roussenova,[†] Mathieu Murith,[‡] Ashraf Alam,[†] and Job Ubbink*[,§]

H. H. Wills Physics Laboratory, University of Bristol, Tyndall Avenue, Bristol BS8 1TL, United Kingdom, Nestlé Research Center, Vers-chez-les-Blanc, CH-1000 Lausanne 26, Switzerland, and Food Concept & Physical Design, Mühleweg 10, CH-4112 Flüh, Switzerland

Received May 7, 2010; Revised Manuscript Received September 25, 2010

The molecular packing of amorphous maltodextrin-glycerol matrices is systematically explored by combining positron annihilation lifetime spectroscopy (PALS) with thermodynamic measurements and dilatometry. Maltodextrin−glycerol matrices are equilibrated at a range of water activities between 0 and 0.54 at $T = 25$ °C to analyze the effect of both water and glycerol on the average molecular hole size and the specific volume of the matrices. In the glassy state, glycerol results in a systematic reduction of the average molecular hole size. In contrast, water interacts with the carbohydrate matrix in a complex way. Thermodynamic clustering theory shows that, at very low water contents the water molecules are well dispersed and are closely associated with the carbohydrate chains. In this regime water acts as an antiplasticizer, whereby it reduces the size of the molecular holes. Conversely, at higher water contents, while still in the glassy state, water acts as a plasticizer by increasing the average hole volume of the carbohydrate matrices. This plasticization-dominated mechanism is likely to be due to the interplay between the ability of water to form hydrogen bonds with the hydroxyl residues on the carbohydrate chains and its mobility, which is significantly decoupled from the bulk mobility of the matrix. Our findings are of key importance for the understanding of the effect of glycerol on the biostabilization performance of these carbohydrate matrices, as it provides a first insight on how molecular packing can relate to the dynamics in such matrices.

Introduction

Various technologies have been developed for the stabilization of sensitive bioactive compounds for the use in foods and pharmaceutics.[1−3] One of the most promising approaches is to encapsulate the bioactive compound in amorphous carbohydrates in the glassy state. This can be achieved by freeze-drying or spray-drying a moderately concentrated solution of an appropriate carbohydrate or a carbohydrate blend, which in addition contains the compound to be protected. One of the central issues in the design of an optimal encapsulating material is the molecular mobility through the matrix (determining its barrier properties), which may allow the escape of the bioactive or inward migration of surrounding molecules (e.g., oxygen or water). The former would lead to premature release of the bioactive, while the latter may degrade the bioactive via chemical reactions.

Initially it was invoked that molecular mobility and therefore stability was primarily related to the difference in temperature between the glass transition temperature (T_g) of the encapsulating matrix and the storage temperature.[2,4] This concept, however, is not universal to all systems, and it is now well recognized that molecular mobility in such materials is not governed by the proximity to the glass transition alone. In particular, it has been shown that the addition of small quantities of specific low-molecular weight compounds to matrices consisting of a carbohydrate of higher molecular weight improves the storage stability of glass-encapsulated bioactives while lowering the glass transition temperature. Several effective combinations of plasticizers and carbohydrates have been found, including glycerol and trehalose,[5] sucrose and maltodextrin, and low-molecular weight starch hydrolysis products (glucose, maltose, and maltotriose) and maltodextrin.[6]

The molecular mobility is predicted to be related to the so-called molecular free volumes, which naturally exist in biopolymer matrices due to their disordered nature. The mechanisms that govern the relationship between the nature of these molecular free volumes and the barrier properties of these materials are, however, still largely unknown. The first step toward the elucidation of the effect of the matrix composition on the barrier properties is, therefore, to establish the relation between matrix composition and matrix free volume.

In our recent PALS studies,[4,7−9] we have shown that the molecular organization of amorphous carbohydrate matrices in the glassy state is strongly influenced by carbohydrate composition and water content. A complex behavior was observed, in particular, as a function of the water content. In the glassy state, at very low water contents, the average molecular hole size decreases with increasing water content, which was explained by a "hole filling" mechanism.[4,7−9] Conversely, at higher water contents, water interacts with the carbohydrate molecules via a plasticization-dominated mechanism.[6−9] Properties relating to the plasticization and antiplasticization of glassy carbohydrates by water have also been widely studied by pressure−volume−temperature (PVT) analysis,[10] nuclear magnetic resonance spectroscopy,[11,12] neutron scattering,[13] infrared spectroscopy,[11,14] and other techniques.[15,16]

Structurally different behavior is observed if, instead of water, low molecular weight disaccharides are added to the carbohydrate matrices.[8,9] The effect of these low molecular weight

* To whom correspondence should be addressed. E-mail: job.ubbink@themill.ch.
[†] University of Bristol.
[‡] Nestlé Research Center.
[§] Food Concept & Physical Design.

10.1021/bm1005068
Published on Web 11/04/2010

plasticizers on the molecular packing of carbohydrate matrices is less complex, leading to a monotonous reduction of the molecular hole size in the glassy state. These additives therefore act as packing enhancers, which could explain the improved glassy-state barrier properties and encapsulation performance of carbohydrate blends containing a low-molecular weight carbohydrate constituent.[6,17]

We interpreted the decrease in hole size with increasing maltose or water contents as antiplasticization. This, however, needs some further clarification because antiplasticization is commonly related to the increase of the elastic moduli of amorphous polymers upon the addition of an antiplasticizer.[18] Furthermore, antiplasticization is also considered to alter the dielectric relaxation dynamics[19] of amorphous polymers and also leads to changes in various other physical properties, such as gas permeation[20] and vapor sorption.[10,21] The precise physical mechanism of antiplasticization is not fully understood, but it is likely to depend on the specific molecular properties of the polymer and the antiplasticizer. Antiplasticization is commonly observed in strongly interacting polymer−diluent systems, where the diluent is a weak plasticizer. This phenomenon is, thus, likely to be related to the gradual disappearance of the β-relaxation upon addition of the diluent.[18,20,22] In line with our interpretation based on the decrease of the molecular hole size, antiplasticization has been interpreted as the reduction of the free volume of the matrix upon addition of the antiplasticizer.[10] For example, Benczédi et al. have previously shown that the role of free volume in the antiplasticization of thermoplastic starch by water may be analyzed using an equation-of-state approach.[10]

In this paper, we take our investigations a significant step forward by extending our studies to a system commonly used in biostabilization which is produced by the addition of glycerol, a low molecular weight polyol, to maltodextrin matrices. In particular, glycerol has been found to enhance the storage stability of proteins encapsulated in matrices consisting of the disaccharide trehalose.[5,13] Glycerol was found to suppress the so-called "fast dynamics" of the glassy trehalose matrices,[13,23] whereby improving their biostabilization performance. As it has been observed that glycerol reduces the mean square amplitude of the molecular vibrations of trehalose in the glassy state, it is of interest to investigate the impact of glycerol on the molecular free volume in glassy carbohydrates. Apart from being widely used as a plasticizer and humectant in foods and pharmaceutics, glycerol is also of interest as its molecular size lies in between that of water and of the disaccharide maltose, which was used in our previous studies as a glassy-state packing enhancer.[8,9] The principal objective of this study is to investigate the mechanism by which glycerol affects the molecular packing and physical properties of maltodextrin matrices, which provides a novel insight to establishing a direct correlation between the nature of the free volume and the barrier- and biostabilization properties of these materials.

For this purpose, we prepared a series of freeze-dried maltodextrin−glycerol matrices with a systematic variation in blend composition and water activity. We combine PALS and specific volume measurements with a thermodynamic characterization of the system (including analysis of the glass transition temperatures and the sorption of water by the matrices). Furthermore, in a related study,[24] Fourier-transform infrared spectroscopy is utilized in conjunction with PALS to investigate the interplay between hydrogen bonding and molecular packing in the glassy carbohydrate matrices.

Table 1. Molecular Weight of the Maltodextrin DE 12 Samples and the Content of Glucose (DP = 1), Maltose (DP = 2), and Maltotriose (DP = 3)

M_n[a,b] (Da)	M_w[a,c] (Da)	$Q_{DP=1}$[d]	$Q_{DP=2}$[d]	$Q_{DP=3}$[d]
1.9×10^3	1.9×10^4	0.009	0.028	0.048

[a] The molecular weight distribution is determined by gel permeation chromatography with pullulan molecular weight standards. [b] Number-average molecular weight. [c] Weight-average molecular weight. [d] Weight fractions determined by high-pressure liquid chromatography.

Theoretical Aspects

One important structural aspect of amorphous systems, such as the carbohydrate−glycerol−water matrices studied in this paper, is the unoccupied volume, which exists between molecules due to irregular molecular packing, density fluctuations, and topological constraints. The unoccupied volume is distributed over local empty volumes (commonly referred to as "holes") of different shapes and sizes. The size of these holes can be probed using PALS by determining the average lifetime or the lifetime distribution of positronium in its long-lived state. In the PALS analysis we assume that the holes are spherical and that the hole size distribution is monodisperse. The unoccupied specific volume then becomes

$$V_{sp,unocc} = N_h v_h \tag{1}$$

where N_h is the number density of holes and $v_h = 4/3\pi r_h^3$ is the volume of a hole with radius r_h.

The specific volume, V_{sp}, of a system may be partitioned between occupied and unoccupied volumes

$$V_{sp} = V_{sp,occ} + V_{sp,unocc} \tag{2}$$

where $V_{sp,occ}$ is the occupied specific volume. The specific volume and its temperature dependence are commonly determined from pressure−volume−temperature (PVT) experiments.[4] The number density of holes may in turn be determined by relating the unoccupied specific volume to the total specific volume of a system, assuming the number density of holes is independent of temperature.[4] It is evident from eqs 1 and 2, however, that the partitioning of the specific volume between the occupied and the unoccupied volumes is not constant, as it depends on the number density and size of the holes.

For a system in thermodynamic equilibrium, the molecular packing and the density, ρ, are completely determined by the thermodynamic variables temperature and pressure, as well as the composition of the system. The matrices studied here are essentially ternary systems made up of maltodextrin, glycerol, and water. However, it should be noted that, strictly speaking, maltodextrin does not constitute a single pure component but rather a distribution of chemically similar components of various molecular weights (Table 1).

The composition of the ternary system may be expressed in terms of weight fractions

$$Q_{md} = \frac{m_{md}}{m_{md} + m_g + m_w};$$
$$Q_g = \frac{m_g}{m_{md} + m_g + m_w};$$
$$Q_w = \frac{m_w}{m_{md} + m_g + m_w} \quad (3)$$

where Q_{md}, Q_g, Q_w, denote the weight fraction of maltodextrin, glycerol and water, and m_{md}, m_g, and m_w the respective masses of the components, respectively.

For a defined blend composition of maltodextrin and glycerol, the water content may vary as the volatility of water remains substantial even at low concentrations. In response to an externally applied water activity, the matrices will therefore take up or release water until thermodynamic equilibrium is achieved. The water vapor sorption isotherms are therefore of fundamental importance in understanding the properties of the maltodextrin−glycerol matrices. When constructing water vapor sorption isotherms, it is customary to express the water content as the ratio of sorbate to sorbent,[25] which is commonly referred to as the water content on a dry basis

$$Q'_w = \frac{m_w}{(m_{md} + m_g)} \quad (4)$$

Because the water content, and therefore the composition of the matrices vary during the sorption process, it is also useful to express the glycerol content on basis of the dry matter:

$$Q'_g = \frac{m_g}{(m_{md} + m_g)} \quad (5)$$

The process of water vapor sorption is rather complicated and several physical regimes have been identified.[26] At high water contents, where the carbohydrates are either in the rubbery state or in the form of aqueous solutions, the sorption of water is well described by liquid-state models such as the Flory−Huggins theory.[27] For low water contents, however, the carbohydrates are in the glassy state and the system becomes nonergodic. In this regime, liquid-like approaches for the sorption of water vapor consequently fail. The water vapor sorption rather resembles the sorption on a rigid adsorbate with a heterodisperse distribution of adsorption sites,[6,10] which may in the simplest form be described by the Freundlich equation[28]

$$Q'_w = k_F \cdot a_w^{1/c} \quad (6)$$

where k_F and c ($c \geq 1$) are temperature-dependent constants representative of the system.

A great deal of effort has been devoted to the evaluation of empirical sorption isotherm models, which can describe the water sorption by amorphous carbohydrate matrices over a wide range of water activities. From the various models, the so-called Guggenheim−Anderson−de Boer (GAB)[29,30] isotherm, which is an adaptation of the multilayer adsorption model of Brunauer, Emmett, and Teller,[29,30] has turned out to be the most useful for the fitting of water vapor sorption data by amorphous carbohydrates

$$Q'_w = \frac{KCW_m a_w}{(1 - Ka_w)(1 - Ka_w + KCa_w)} \quad (7)$$

where K, C, and W_m are constants characterizing the system.

Upon changes in water content, the carbohydrate matrix may either expand or shrink, leading to a change in specific volume. The degree of volumetric swelling by the uptake or release of water is defined by[6]

$$\theta = \frac{V}{V_0} = \frac{\rho_0}{\rho} \cdot \frac{1}{Q_{org}} \quad (8)$$

where the subscript "0" refers to the dry state, and $Q_{org} = Q_{md} + Q_g = 1 - Q_w$, is the weight fraction of organic matter, where Q_{md}, Q_g, and Q_w are defined in eq 3.

Useful information about the overall distribution of water molecules in the matrices may be obtained by analyzing the water vapor sorption isotherms and the specific volume of the system in terms of the Zimm−Lundberg clustering theory.[31] This formalism makes use of the cluster integral, which is the positional average of the pair distribution function F_2, for two water molecules with coordinates i and j, defined by

$$G_{ww} = \frac{1}{V}\int\int (F_2(i,j) - 1)\mathrm{d}i\mathrm{d}j \quad (9)$$

The cluster integral for two water molecules in the carbohydrate matrix can be related to the water activity of a carbohydrate polymer matrix via the clustering function

$$\frac{G_{ww}}{\bar{v}_w} = -\phi_{v,org}\left[\frac{\partial(a_w/\phi_{v,w})}{\partial a_w}\right]_{T,p} - 1 \quad (10)$$

where $\phi_{v,w}$ and $\phi_{v,o} = \phi_{v,m} + \phi_{v,g}$ signify the volume fraction of water and organic matter, respectively, and $\bar{v}_w$ is the partial molar volume of water in the system.[32,33] Eq 10 is valid as long as the compressibility of the system is negligible. The average number of water molecules clustering around any individual water molecule in excess of the mean concentration of water molecules is $\phi_{v,w}G_{ww}/\bar{v}_w$. Positive values of the clustering function indicate that water in the carbohydrate matrix forms small clusters or "pockets" between the carbohydrate chains. Conversely, negative values of the clustering function signify that water is molecularly dispersed in the carbohydrate matrix. The state $G_{ww}/\bar{v}_w = -1$ represents a random distribution of noninteracting water molecules.

Materials and Methods

Preparation of Matrices. Maltodextrin DE 12 (Glucidex IT-12, 98% purity) was obtained from Roquette Frères (Lestrem, France). The molecular weight characterization is summarized in Table 1. Maltodextrins are the products of the controlled hydrolysis of starch, and are mixtures of α(1→4) linked glucose oligo- and polysaccharides with occasional α(1→6) branches.[34,35] The degree of hydrolysis of the maltodextrins is indicated by the dextrose equivalence (DE) value,[34] which denotes the percentage fraction of reducing sugars in the sample (DE value of nonhydrolyzed starch is below 1, DE 100 is equivalent to glucose). The DE value therefore reflects the number-average molecular weight of the carbohydrate. Matrices of varying maltodextrin−glycerol composition were prepared by dissolving the correct

weight fractions of glycerol (87% purity, Fluka, Buchs, Switzerland) and maltodextrin in ultrapure water (Milli-Q, Millipore, Beford MA, U.S.A.) at 25 °C. Blends were prepared with $Q'_g = 0$, 0.02, 0.06, 0.10, 0.15, and 0.20. These glycerol weight fractions were corrected for water contained in the glycerol product used. All materials were used without further purification. The solutions, all at a water content of 70 ± 1 wt %, were subsequently heated to $T = 60$ °C, and stirred for 30 min using a magnetic stirrer. The matrices were then prepared by freeze-drying these solutions overnight using a LD85 freeze-dryer (Millrock Technologies, Kingston, NY). The temperature profile during freeze-drying started at $T = -50$ °C and was increased in a stepwise manner to $T = 25$ °C, taking care not to exceed the glass transition temperature of the matrices. The freeze-dried powders were then carefully ground and equilibrated at set water activities in desiccators containing saturated salt solutions. The samples for the PALS experiments were prepared by compaction of about 0.12 g of water activity equilibrated powder into disks (diameter 1 cm, thickness 1.1 mm) using a laboratory press.

Water Activity Equilibration. Samples were equilibrated at $T = 25$ °C at various water activities in desiccators containing a dessicant or saturated salt solutions of known relative humidity ($a_w = 0$ (P_2O_5), 0.11 (LiCl), 0.22 (CH_3COOK), 0.33 ($Mg Cl_2$), 0.43 (K_2CO_3), and 0.54 ($Mg(NO_3)_2$) ($T = 25$ °C)).[36] The sorption of water was followed gravimetrically until equilibrium was achieved (generally within 25 days).

Measurement of Water Activity and Water Content. The initial water activity of the samples was measured in duplicate with a humidity sensor (Hygroscop DT, Rotronic AG, Switzerland) kept at $T = 25 \pm 0.1$ °C and calibrated with saturated salt solutions of known humidity (see above). The water content was determined in duplicate using a home-built extraction unit, as described previously.[6]

Positron Annihilation Lifetime Spectroscopy (PALS) Experiments and Analysis. Positron annihilation lifetime experiments were performed using a fast−fast coincidence system with a Gaussian resolution function having a full width at half-maximum (fwhm) of 0.175 ns. Full details of the system are described elsewhere.[4] ^{22}Na was used as the source of positrons, and it was prepared by depositing aqueous NaCl between two 7.5 μm sheets of Kapton foil. ^{22}Na was used as positron source as it decays to ^{22}Ne with a prompt emission of a 1.28 MeV gamma ray, which can be used to register the "birth" of the positron. The sample disks were placed on either side of the source and the sample cavity was filled with powder equilibrated at the same water activity as the sample, to minimize water vapor within the airtight copper sample cell (described in ref 6). The thickness of the sample disks was ~1.1 mm, enough to stop ~99% of the positrons. The spectra were collected over a minimum period of two hours to generate at least 2 million events per spectrum, unless stated otherwise. The source correction was 8.8% of the total spectrum, with two components measured, 0.38 ns ($I = 91.2\%$) and 2.94 ns ($I = 8.8\%$). These were removed from the spectra prior to the analysis.

PALS experiments proceed by injecting a positron into the material being tested and measuring the length of time until that positron annihilates with one of the material's electrons, producing γ rays. When a positron enters a molecular material it thermalizes within a few picoseconds.[37] After this, it may diffuse through the material over a mean free path of a few nm, either as a free particle and self-annihilate directly (in a time period of ~0.4 ns, producing two 511 keV γ rays), or capture an electron to form a Ps atom. Ps is an electron−positron bound state with a binding energy of 6.8 eV in vacuum, although it may be less in media.[38] Ps has two spin states: *para*-positronium (*p*-Ps), a singlet state with zero spin angular momentum; and *ortho*-positronium (*o*-Ps), a triplet state of unit spin angular momentum. In vacuum, *p*-Ps self-annihilates to two 511 keV γ rays in 0.125 ns, whereas *o*-Ps due to spin considerations can only self-annihilate to an odd number of photons (three being the most probable), with an average lifetime of 142 ns. In molecular materials, once formed, Ps localizes in the free volume holes between the molecules, where it remains throughout its lifetime. As a consequence of the collisions of *o*-Ps with the "walls" of the hole in which it resides, the *o*-Ps's positron can annihilate with an electron with an opposite spin, other than its bound partner. This is known as "pick-off" annihilation, which results in a decrease of the *o*-Ps lifetime with hole size, from 142 ns in an infinite size hole (*o*-Ps self-annihilation in vacuum) to the low nanosecond range for subnanometer sized holes. The *o*-Ps lifetime is, therefore, environment dependent and it delivers information pertaining to the size of the molecular free volumes in a material. Assuming that the holes are spherical in shape, a semiempirical model[39,40] can be used to relate the *o*-Ps pick-off lifetime, τ_{po}, to the size of the hole radius, r_h, via the so-called Tao−Eldrup equation[38,39]

$$\tau_{po} = 0.5\,\text{ns}\left[1 - \frac{r_h}{r_h + \delta r} + \frac{1}{2\pi}\sin\left(\frac{2\pi r_h}{r_h + \delta r}\right)\right]^{-1} \quad (11)$$

The 0.5 ns is the spin-averaged lifetime of the Ps, and the empirically determined $\delta r = 1.66$ Å[39] describes the penetration of the Ps wave function into the hole "walls". Conventionally, the lifetime spectra are decomposed into three discrete exponential components

$$S(t) = \left[R(t) \otimes \sum (I_i/\tau_i)\exp(-t/\tau_i)\right] + B \quad (12)$$

where $i = 1, 2, 3$ are the components attributed to the annihilation of *p*-Ps, free positron, and *o*-Ps, respectively, weighted by the relevant intensity I_i (where $\sum I_i = 1$). B is the background and $R(t)$ is the resolution function, where t is time. Here, for the lifetime analysis we use the nonlinear least-squares fitting routine Life Time[41] in its latest version LT 9.1.[42]

Density Measurements. The density of the samples, ρ, was determined using an Accupyc 1330 pycnometer (100 mL cell with 10 mL insert; Micrometrics, U.S.A.) as previously described.[4]

Table 2. Glass Transition Temperatures of the Maltodextrin Matrices with Various Glycerol Contents Equilibrated at a Range of Water Activities between $a_w = 0.11$ and $a_w = 0.54$ ($T = 25$ °C)[a]

	T_g (°C)				
Q'_g	$a_w = 0.11$	$a_w = 0.22$	$a_w = 0.33$	$a_w = 0.43$	$a_w = 0.54$
0.00	106 ± 4	78 ± 7	71 ± 3	65 ± 6	46 ± 6
0.02	86 ± 5	68 ± 5	55 ± 3	45 ± 4	32 ± 4
0.06	69 ± 5	49 ± 4	40 ± 4	37 ± 2	25 ± 4
0.10	55 ± 6	40 ± 5	23 ± 6	21 ± 3	7 ± 3
0.15	35 ± 3	22 ± 4	15 ± 6	2 ± 4	−9 ± 3
0.20	13 ± 4	5 ± 2	−1 ± 2	−15 ± 2	−21 ± 4

[a] T_g is defined as the temperature of intersection of the linear regression of the PALS data in the rubbery and the glassy states. The standard errors for all T_g measurements are reported in the table.

Results and Discussion

Thermodynamic Characterization. In the subsequent treatment, a distinction needs to be made between samples, which are in the glassy state from those that are in the rubbery state, therefore, we first quantify the effect of water on the glass transition temperature (T_g) of the various maltodextrin−glycerol matrices. The glass transition temperature of the matrices is commonly determined using differential scanning calorimetry (DSC). In the present investigation, T_g was, however, determined from temperature-dependent PALS measurements, following a procedure which is discussed below. It has been shown that the values of T_g determined from PALS measurements are in excellent agreement with those obtained by DSC.[4] The glass transition data (Table 2) are fitted to the semiempirical Gordon−Taylor equation[43,44]

$$T_g = \frac{Q_{org}T_{g,org} + k_{GT}Q_wT_{g,w}}{Q_{org} + k_{GT}Q_w} \quad (13)$$

where $Q_{org} = Q_{md} + Q_g$ is the weight fraction of organic compounds (maltodextrin and glycerol), Q_w is the water content on a wet basis, $T_{g,w}$ is the glass transition temperature of water ($T_{g,w} = -134$ °C[45]), $T_{g,org}$ is the glass transition of the anhydrous carbohydrate−glycerol matrix, and k_{GT} is the Gordon−Taylor coefficient. When modeling the experimental data, both $T_{g,org}$ and k_{GT} are considered as fitting parameters. The fitting coefficients reported in Table 3 are within the range reported for similar systems.[6,26,46−48]

To distinguish between the glassy and the rubbery states for the experiments that are performed at room temperature, the critical water content, Q_w*, at which the glass transition temperature equals $T = 25$ °C is determined from the Gordon−Taylor fits (Table 3). Q_w* decreases as a function of glycerol content from 0.13 for the matrix containing 0 wt % glycerol to 0.03 for the matrix containing 20 wt %. glycerol (Figure 1). The critical water activities, a_w*, corresponding to Q_w* are also given in Table 3. With increasing glycerol content, the value of a_w* decreases from 0.67 for the matrix containing 0 wt % glycerol to 0.08 for the matrix containing 20 wt % glycerol, confirming the plasticizing effect of glycerol on the carbohydrate matrices.

In Figure 2a, the water vapor sorption isotherms in the water activity range $a_w = 0$ to $a_w = 0.54$ are shown for the various maltodextrin−glycerol matrices ($T = 25$ °C). For the samples at the higher glycerol contents, the characteristic sigmoidal water sorption behavior, which is related to the transition from the glassy to the rubbery state, is observed.[26] As expected, the sorption data are well fitted by the GAB isotherm model[29] (see Table 4). This model, due to its descriptive rather than mechanistic nature, must be treated with caution.[26] For this reason, we also use the Freundlich isotherm model (eq 6) to fit the sorption data of the matrices but only in the glassy state (see Table 5). The Freundlich model, which has a certain physical foundation for the sorption on energetically heterogeneous sites,[10] was previously shown to apply to the sorption of water by carbohydrate matrices in the glassy state.[6,10] In Figure 3a, we observe that the k_F coefficient from the Freundlich model decreases as a function of the glycerol content in the anhydrous state. Interestingly, k_F also shows a positive relationship with the size of the molecular free volumes of the maltodextrin matrices (Figure 3b). This highlights the importance of molecular packing for the sorption of water in these systems. The more densely packed the matrices are, the less space available there is to accommodate water molecules. Consequently, less water can be absorbed by the glassy matrices at a defined water activity. Similar relations between k_F and the specific and hole volumes were previously found for blends of a fractionated maltopolymer and maltose.[9,26] The current results are, however, of interest, as they extend this earlier finding to blends that consist of chemically quite disparate components. The value of the constant c of the Freundlich equation is found to be essentially independent of the matrix composition, in agreement with previous studies on similar systems.[26] Its mean value ($c = 1.80$) was therefore used in fitting the experimental data. It is of interest to note that sub-T_g aging of a glassy matrix may reduce the amount of water absorbed at a given water activity (still in the glassy state).[49] This could be related to changes in density and hole volume during the aging process. However, no quantitative analysis of such aging-dependent sorption in relation to structural rearrangements are currently available. One should also be aware that, because the long duration of typical sorption experiments, there is a complex interdependency between water vapor sorption and glassy state matrix aging.

Table 3. Fitting Parameters of the Gordon−Taylor Equation (Eq 13) for the Various Maltodextrin−Glycerol Matrices[a]

Q'_g	$T_{g,org}$ (°C)[b]	k_{GT}	Q_w*[c]	a_w*[d]
0.00	198 ± 6	7.2 ± 0.4	0.13	0.67
0.02	179 ± 5	8.2 ± 0.4	0.11	0.56
0.06	143 ± 5	8.1 ± 0.6	0.08	0.48
0.10	116 ± 5	8.5 ± 0.6	0.06	0.37
0.15	87 ± 5	7.6 ± 0.6	0.05	0.24
0.20	63 ± 6	7.4 ± 0.7	0.03	0.08

[a] All standard errors for the fitting parameters are reported in the table. [b] Glass transition temperature of the anhydrous carbohydrate matrix following the fit of the data to the Gordon−Taylor equation. [c] Weight fraction of water. [d] Water activity at which the glass transition temperature of the carbohydrate matrix is 25 °C.

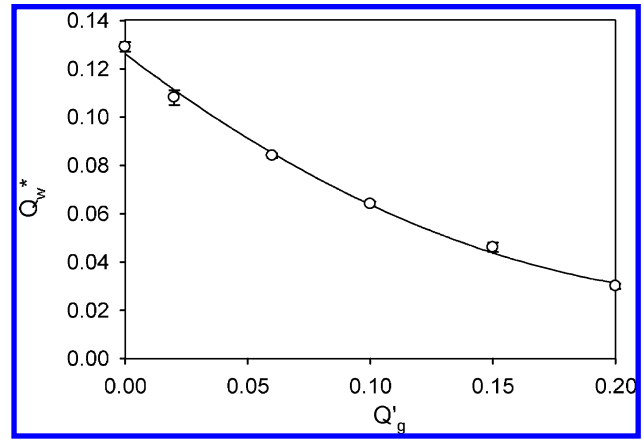

Figure 1. Critical water content at which $T_g = 25$ °C (Q_w*) for the maltodextrin matrices as a function of glycerol content. The Q_w* values were calculated from the fits of the glass transition temperature data (Table 2) to the Gordon−Taylor equation (eq 13).

Similar trends hold for the fitted values for the coefficients, W_m and C (related to the free energy of sorption at low partial pressure,[28] but also to the shape of the isotherm at values of the water activity close to unity) from the GAB isotherm model. The value of the coefficient C was found to be virtually independent of the glycerol content. In the fits presented in Figure 2a and in Table 4, its value was therefore fixed to $C = 15.7$, the average value obtained from a free fit of the water vapor sorption data for different matrix compositions.

From Figure 2a, it is also clear that the sorption behavior of the matrices is dependent on the glycerol content below and above T_g. This is depicted more clearly in Figure 2b, where the sorption data are replotted as a function of the glycerol content at a constant water activity. In the rubbery state, the amount of water absorbed by the matrices rapidly increases as a function of glycerol content at a constant water activity, whereas in the glassy state we observe the opposite trend. This behavior, which has been previously reported for similar systems,[26,50] can be related to the entropy of mixing of the constituent molecules in the rubbery state and to the molecular packing in the glassy state. For the maltodextrin−glycerol systems, the effect of the physical state on the water sorption is somewhat less pronounced than for the maltopolymer−maltose systems studied before.[26] It is also worth mentioning that the results reported by Enrione et al.[50] on the sorption behavior of a starch−glycerol system may also be interpreted in terms of the two-state model described in ref 26.

The Zimm−Lundberg clustering function for water molecules, which is calculated from the water sorption data (Figure

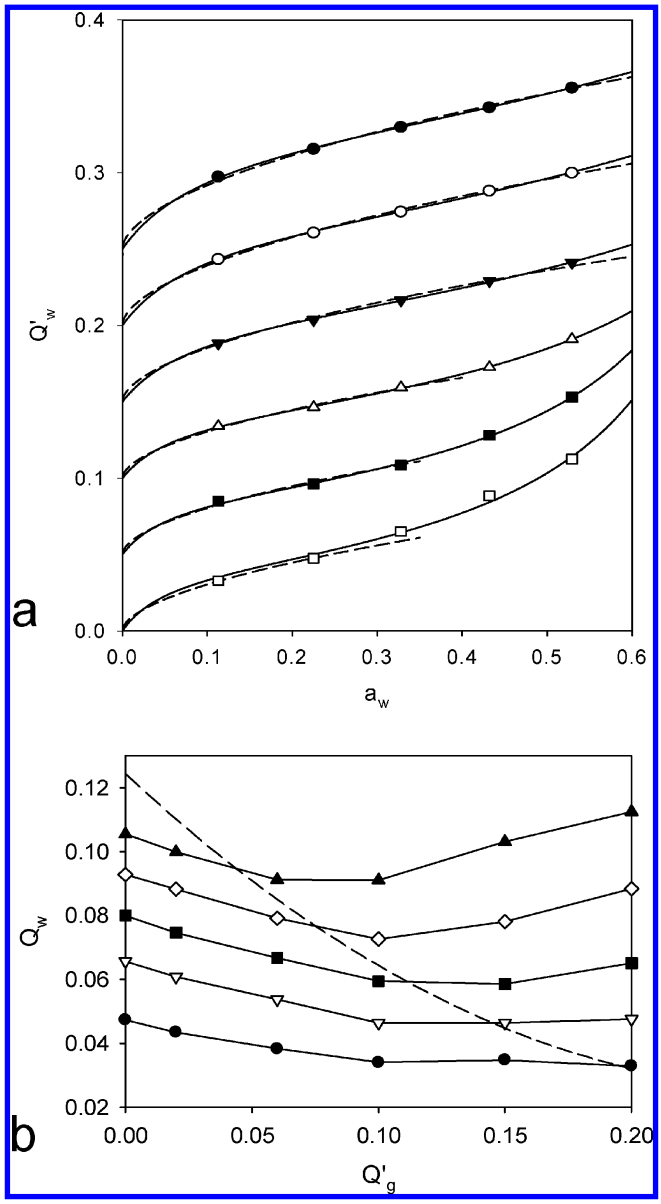

Figure 2. (a) Water vapor sorption isotherms for the matrices at $T = 25$ °C as a function of glycerol content. The solid and dashed lines represent the optimal fit using the GAB model and the Freundlich model, respectively. The fitting coefficients are reported in Table 4 for the GAB model and in Table 5 for the Freundlich model. Filled circles, $Q'_g = 0$; open circles, $Q'_g = 0.02$; filled triangles, $Q'_g = 0.06$; open triangles, $Q'_g = 0.10$; filled squares, $Q'_g = 0.15$; open squares, $Q'_g = 0.20$. The sorption isotherms for the matrices at $Q'_g = 0.00$, $Q'_g = 0.02$, $Q'_g = 0.06$, $Q'_g = 0.10$, and $Q'_g = 0.15$ are shifted vertically by 0.25, 0.20, 0.15, 0.10, and 0.05 units, respectively. (b) Water content as a function of the glycerol weight fraction for the matrices equilibrated at various water activities ($T = 25$ °C). The dashed line (derived from Figure 1) denotes the relation between matrix composition and water content at which $T_g = 25$ °C for the matrices. Filled circles, $a_w = 0.11$; open triangles down, $a_w = 0.22$; filled squares, $a_w = 0.33$; open diamonds, $a_w = 0.43$; filled triangles up, $a_w = 0.54$. The standard error in the reported water content values is ±0.002.

2) and the density data (Table 6) for the matrices, is shown in Figure 4. For all matrices, the clustering functions are strongly negative at low water volume fractions, suggesting that water is present in a highly dispersed state within the matrices. This is commensurate with individual water molecules forming hydrogen bonds with the hydroxyl residues on the maltodextrin chains. As the volume fraction of water is increased further (up

Table 4. Fitted Values for the Parameters of the GAB Isotherm Model (Eq 7) for the Water Vapor Sorption of Maltodextrin Matrices with Different Blend Compositions[a]

Q'_g	K	W_m	residue[b]
0.00	0.66 ± 0.02	0.08 ± 1 × 10^{-3}	1.0 × 10^{-6}
0.02	0.72 ± 0.03	0.07 ± 2 × 10^{-3}	1.9 × 10^{-6}
0.06	0.79 ± 0.02	0.06 ± 1 × 10^{-3}	1.5 × 10^{-6}
0.10	1.02 ± 0.01	0.05 ± 1 × 10^{-3}	1.4 × 10^{-6}
0.15	1.18 ± 0.02	0.04 ± 1 × 10^{-3}	5.5 × 10^{-6}
0.20	1.21 ± 0.03	0.04 ± 2 × 10^{-3}	5.4 × 10^{-6}

[a] As discussed in the text, the value of C was fixed to 15.7. All standard errors for the fitting coefficients are reported in the table. The sorption data ($T = 25$ °C) are fitted over the interval $0 \le a_w \le 0.54$. [b] $\sum_n (Q'_{exp,n} - Q'_{model,n})^2$.

Table 5. Fitted Values for the Coefficient k_F of the Freundlich Isotherm Model (Eq 6) for the Water Vapor Sorption of Maltodextrin Matrices with Different Blend Compositions[a]

Q'_g	k_F	a_w range[b]	residue[c]
0.00	0.15 ± 1 × 10^{-3}	0.00−0.54	8.2 × 10^{-6}
0.02	0.14 ± 1 × 10^{-3}	0.00−0.54	5.2 × 10^{-6}
0.06	0.12 ± 1 × 10^{-3}	0.00−0.43	2.6 × 10^{-6}
0.10	0.11 ± 2 × 10^{-3}	0.00−0.33	4.2 × 10^{-6}
0.15	0.11 ± 2 × 10^{-3}	0.00−0.11	6.5 × 10^{-6}
0.20	0.11 ± 1 × 10^{-3}	0.00−0.11	1.7 × 10^{-6}

[a] As discussed in the text, the value of c was fixed to 1.80. Standard errors for the coefficient k_F are reported in the table. [b] The sorption data ($T = 25$ °C) for each matrix composition are fitted over the water activity intervals stated. [c] $\sum_n (Q'_{exp,n} - Q'_{model,n})^2$.

to $\phi_{v,w} \sim 0.06$), the values of the clustering function increase, while still remaining negative, suggesting that water is still localized in the vicinity of the carbohydrate chains. It is also clear that, at a constant volume fraction of water, the clustering function increases as a function of the glycerol content. At these somewhat higher volume fractions of water, we observe a clear difference between the samples, which remain in the glassy state compared to those, which become rubbery. For the samples that become rubbery ($Q'_g = 0.10$, 0.15, and 0.20), the clustering function continues to increase rapidly and levels off only at positive values. For the samples that remain glassy over the full water activity range (up to $a_w = 0.54$), the values of the clustering function increase significantly less rapidly as a function of the volume fraction of water and, thus, remain negative even at the highest water activities studied. Our interpretation is that as the matrices enter the rubbery state, small clusters of water begin to form. Consequently, in the rubbery state, the degree of association of the water molecules with the maltodextrin chains is different compared to this in the glassy state. In line with the results from molecular dynamics simulations of carbohydrate−water systems,[51] we anticipate that, in the rubbery state, the degree hydrogen bonding is lower and the hydrogen-bond lifetimes are significantly shorter.

Structure of the Local Free Volume from PALS. To elucidate the effect of glycerol on the molecular packing of the maltodextrin matrices, we first plot the dependence of the molecular hole volume on the matrix composition, for samples equilibrated at $a_w = 0.33$ and $a_w = 0.54$ (Figure 5). Here, we present PALS measurements for thermally annealed samples, starting from the rubbery state on descending temperature runs. We ensured identical thermal histories for all samples by initially heating them to $T_g + 50$ °C for several hours (to erase their previous thermal histories) and then subjecting them to identical cooling cycles consisting of quasi-isothermal steps.

In the analysis of the PALS data, it is assumed that the distribution of the hole volumes is monodisperse, even though this is not strictly the case.[8] Although theoretically it is possible

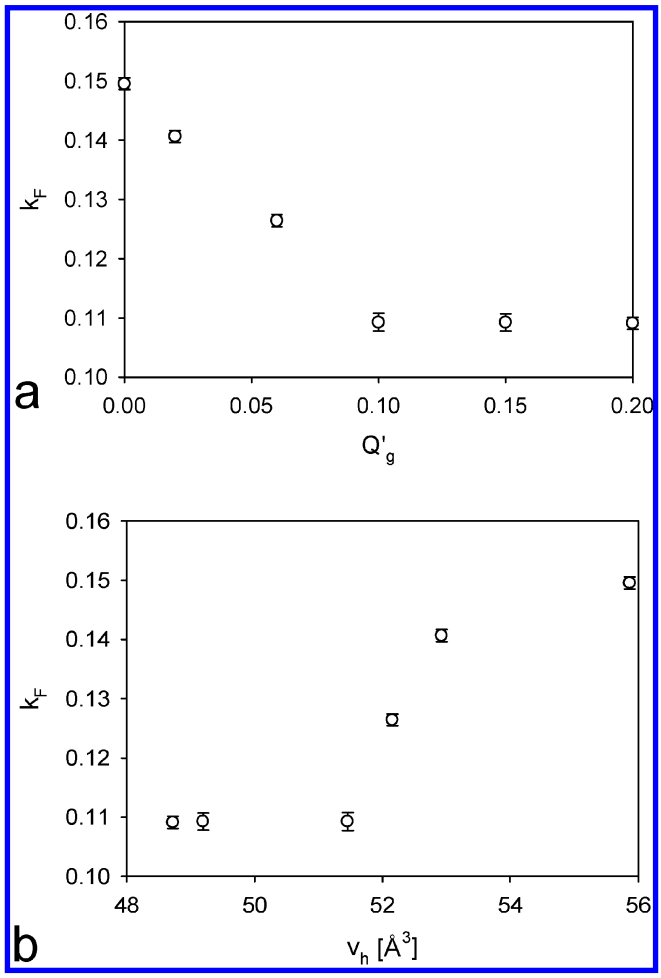

Figure 3. Dependence of the k_F coefficient from the Freundlich isotherm model on (a) the glycerol content and (b) the average hole volume of the anhydrous maltodextrin−glycerol matrices measured at $T = 25$ °C.

to determine the shape of the hole size distribution from PALS measurements, the statistics required to do so can be prohibitively high. The statistics required to determine the hole size distribution in these carbohydrate samples are about 10 times higher than the statistics in the present study. Collection of high statistics spectra also poses experimental issues such as radiation damage, potential instrumental drift, and unfeasibly long experimental time scales. To provide an estimate of the hole-size dispersions in these materials, we present one set of data obtained at relatively high statistics (~5.5 million counts for each measurement). Assuming the *o*-Ps annihilation rate λ ($\lambda = 1/\tau_{po}$) follows a log-normal distribution,[37] the mean and the standard deviation in the *o*-Ps lifetime can be calculated using the program LT9.[41] These variables, used in conjunction with the Tao−Eldrup equation (eq 11), can in turn be used to calculate the number weighted hole volume distribution, the first and second moments of which correspond to the average hole volume, $\langle v_h \rangle$, and the dispersion in the molecular free volume size, σ_h. From Table 7, we can see that the matrices equilibrated at $a_w = 0.33$ show a significant dispersion in hole size, with a standard deviation of ~25.2 ± 0.5 Å^3 for the samples containing glycerol and ~29.3 ± 0.5 Å^3 for the pure maltodextrin matrix. It is of interest to note that the dispersion does not change significantly as a function of the glycerol weight fraction. Consequently, the dispersion of the hole sizes does not convey much additional information about the mechanism by which glycerol alters the molecular packing of the maltodextrin matrices. We may therefore structure our arguments based on the changes in the mean hole size when interpreting the effect of glycerol on the molecular organization of the matrices.

From Figure 5, it is clear that the hole changes as a function of temperature, showing two linear branches, each of which can be fitted well with a linear regression (Tables 8 and 9). Furthermore, the thermal expansion of the hole volume is lower for the low-temperature branch. At low temperatures, the molecules are "frozen" into the glassy state, and the small expansion in the hole volume is due to the anharmonicity of the molecular vibrations in the vicinity of the holes. When the temperature is increased, the samples pass into the rubbery phase, and the hole volume increases more rapidly as the molecules vibrate more freely and at a higher frequency. The thermal expansion of the molecular free volume, both in the glassy and in the rubbery states, is very similar for all matrix compositions (Tables 8 and 9). A significantly different behavior is however, observed for the matrices containing 20 wt % glycerol equilibrated at $a_w = 0.54$ (Figure 5b). This puzzling behavior is most likely not due to phase separation, as suggested by the glass transition temperature of the matrix, which is in line with what is expected based on the glass transition temperatures of the matrices at lower glycerol and water contents.

In Figure 5, the glass transition temperature, T_g, can be identified as the point of intersection of the two temperature branches. A reduction in T_g is observed as a function of the glycerol content for matrices equilibrated at the same water activity (Table 2). The interpretation of Figure 5a and b is, however, complicated by the fact that the water content of matrices equilibrated at the same water activity varies significantly as a function of the glycerol content (Figure 2b). Whereas the fitted coefficients of the Gordon−Taylor equation (eq 13) can be used to obtain the glass transition temperature of the maltodextrin−glycerol matrices at any desired water content (as long as no ice is formed), the relation between the hole volume, the glycerol and water contents would need to be established at a range of temperatures.

The variation in hole size as a function of water content at $T = 25$ °C is plotted in Figure 6 for various maltodextrin−glycerol blend compositions. This reveals complex changes in the hole size of the matrices as a function of the water content, which can be broadly divided into three regimes.

Regime 1. Starting from the fully anhydrous state, the hole volume initially decreases upon sorption of water. The hole volume reaches a minimum, which varies from around $Q_w \sim 0.04$ for the low glycerol content matrices to $Q_w \sim 0.06$ for matrices with higher glycerol contents. The decrease in hole size with increasing water content is more pronounced for the low glycerol content samples, as they are in the glassy state. This reduction in free volume of the carbohydrate matrices by water is most likely related to antiplasticization, an effect reported in refs 6 and 8. Previously, a "hole filling" mechanism was proposed to explain the phenomenon in similar systems.[4,8] This mechanism is rather descriptive and should be treated with caution. The largest reduction in the hole volume observed in this study is for the matrix containing 6 wt % glycerol, with a decrease of 2.60 Å^3, as the water content increases to 0.05 from the anhydrous state. At this water content, we estimate the number density of water molecules to be ~2.8×10^{21} per cubic centimeter. Following the framework set out in ref 4, where the calculated density of holes in a similar carbohydrate matrix was ~1.5×10^{21} cm^{-3}, we estimate that there are, on average, two water molecules per hole. The van der Waals volume of a

Table 6. Density of the Maltodextrin Matrices for Various Blend Compositions at $T = 25$ °C after Annealing above T_g[a]

	ρ (g·cm^{-3})					
a_w (25 °C)	$Q'_g = 0.00$	$Q'_g = 0.02$	$Q'_g = 0.06$	$Q'_g = 0.10$	$Q'_g = 0.15$	$Q'_g = 0.20$
0.00	1.494 ± 0.023	1.492 ± 0.006	1.495 ± 0.007	1.492 ± 0.004	1.488 ± 0.006	1.482 ± 0.008
0.11	1.524 ± 0.007	1.532 ± 0.011	1.545 ± 0.002	1.542 ± 0.002	1.527 ± 0.006	n.d.
0.22	1.567 ± 0.008	1.571 ± 0.001	1.559 ± 5 × 10^{-5}	1.566 ± 0.020	1.561 ± 4 × 10^{-4}	1.542 ± 0.005
0.33	1.566 ± 0.006	1.578 ± 0.018	1.564 ± 0.002	1.571 ± 0.005	1.558 ± 0.007	1.522 ± 0.003
0.43	1.596 ± 0.004	1.586 ± 0.007	1.589 ± 0.008	1.582 ± 0.018	1.577 ± 0.024	n.d.
0.54	1.648 ± 0.014	1.618 ± 0.007	1.612 ± 0.0014	1.595 ± 0.026	n.d.	n.d.

[a] The standard deviation for all measurements is reported in the table. n.d. = not determined.

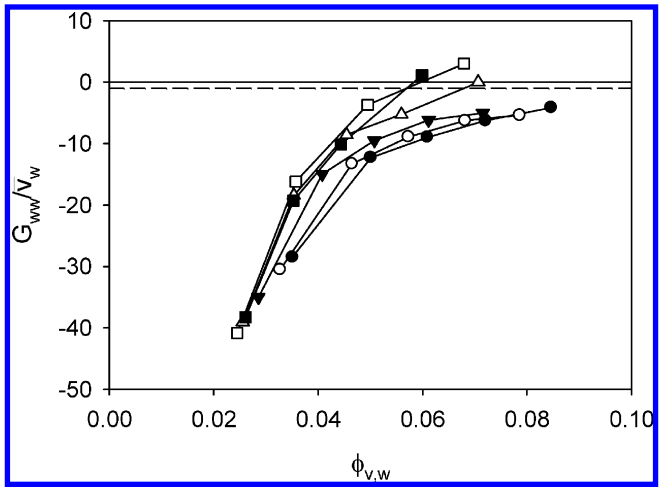

Figure 4. Zimm−Lundberg clustering function for water molecules as a function of the volume fraction of water for maltodextrin matrices with various compositions. The dashed line represents the $G_{ww}/\bar{v}_{ww} = -1$, state, where the distribution of water molecules is random. Filled circles, $Q'_g = 0$; open circles, $Q'_g = 0.02$; filled triangles, $Q'_g = 0.06$; open triangles, $Q'_g = 0.10$; filled squares, $Q'_g = 0.15$, open squares, $Q'_g = 0.20$.

water molecule is 11.7 Å^3,[45] meaning that according to the "hole filling" mechanism we should measure a decrease in hole volume of ~23.4 Å^3. This is about nine times larger than the measured reduction in the hole volume, suggesting that the observed changes in the hole size cannot be explained by a simple "hole filling" mechanism. The reported decrease in hole size is therefore most likely to be due to changes in the local organization and packing of the constituent molecules.

Regime 2. As the water content is further increased, water acts as a plasticizer with a consequent increase in the hole volume, even for matrices in the glassy state. Although the long-range coordinated rearrangements of the maltodextrin chains are frozen out in the glassy state, it has been shown that significant local mobility is still possible.[52] A decoupling of the mobility of water and the carbohydrate molecules is expected close to T_g because the water molecules remain to some extent mobile even in the glassy state.[14,53] An important consequence of the decoupling of the two mobilities is that it allows Arrhenius-type diffusion of water, enabling the water molecules to plasticize their local environment.[53] The mechanism of plasticization is, however, likely to be very complex because of the possible interplay between the mobility of water molecules and their ability to form hydrogen bonds with the hydroxyl residues on the maltodextrin chains. Water−carbohydrate hydrogen bonds may replace some of the carbohydrate−carbohydrate hydrogen bonds, thereby altering the structure of the carbohydrate matrix and creating a more open network. This mechanism is investigated in more detail in a related paper, where we combine PALS and FTIR measurements to simultaneously probe the size of the molecular free volumes and the hydrogen-bonding interactions in these matrices.[24]

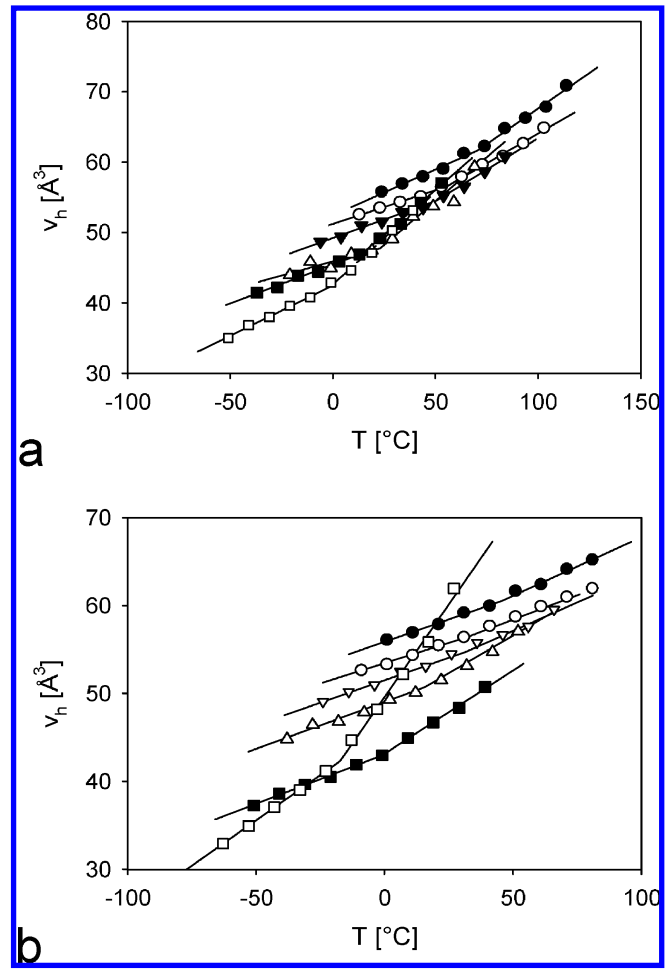

Figure 5. Hole volume as a function of temperature for the annealed maltodextrin matrices with different glycerol contents, equilibrated at (a) $a_w = 0.33$ and (b) $a_w = 0.54$ ($T = 25$ °C). Filled circles, $Q'_g = 0$; open circles, $Q'_g = 0.02$; filled triangles, $Q'_g = 0.06$; open triangles, $Q'_g = 0.10$; filled squares, $Q'_g = 0.15$; open squares, $Q'_g = 0.20$.

Table 7. Mean Hole Volume, $\langle v_h \rangle$, and the Width of the Hole Volume Distribution, σ_h, for Variations in Matrix Composition for Samples Equilibrated at $a_w = 0.33$

Q'_g	0.00	0.02	0.06	0.10	0.15	0.20
$\langle v_h \rangle$ (Å^3)	56.9	55.1	54.1	48.9	49.7	50.6
σ_h (Å^3)	29.3	24.6	26.3	24.3	25.7	24.8

Regime 3. Upon further increase in the water content, the samples become rubbery. In this regime structural rearrangements occur on a time scale of seconds or less and, as noted before, the differences in the void structure between the various blend compositions tend to become smaller (Figure 6).[8] This is particularly evident for the matrix containing 20 wt % glycerol at $Q_w \approx 0.11$. The purpose of this paper is to investigate the

Table 8. Linear Regression of the Temperature-Dependent PALS Data for the Annealed Maltodextrin−Glycerol Matrices Equilibrated at $a_w = 0.33$[a]

Q'_g	$\alpha(T < T_g)$[b] [Å^3·°C^{-1}]	$v_h(T_g)$[c] [Å^3]	$\alpha(T > T_g)$[b] [Å^3·°C^{-1}]
0.00	0.13	62	0.20
0.02	0.10	57	0.17
0.06	0.10	55	0.18
0.10	0.08	48	0.25
0.15	0.11	47	0.25
0.20	0.14	42	0.26

[a] Typical standard errors are $\alpha(T < T_g)$: 0.01 Å^3·°C^{-1}; $\alpha(T > T_g)$: 0.01 Å^3·°C^{-1}; $v_h(T_g)$: 4 Å^3. All correlation coefficients are $R^2 \geq 0.97$. [b] Gradient of the linear regression of the hole volume versus temperature. [c] The glass transition temperatures T_g are reported in Table 2.

Table 9. Linear Regression of the PALS Data for the Annealed Maltodextrin−Glycerol Matrices Equilibrated at $a_w = 0.54$[a]

Q'_g	$\alpha(T < T_g)$[b] [Å^3·°C^{-1}]	$v_h(T_g)$[c] [Å^3]	$\alpha(T > T_g)$[b] [Å^3·°C^{-1}]
0.00	0.10	61	0.13
0.02	0.09	56	0.11
0.06	0.10	54	0.13
0.10	0.11	51	0.17
0.15	0.11	43	0.19
0.20	0.21	42	0.42

[a] Typical standard errors are $\alpha(T < T_g)$: 0.01 Å^3·°C^{-1}; $\alpha(T > T_g)$: 0.01 Å^3·°C^{-1}; $v_h(T_g)$: 4 Å^3. All correlation coefficients are $R^2 \geq 0.97$. [b] Gradient of the linear regression of the hole volume versus temperature. [c] The glass transition temperatures T_g are reported in Table 2.

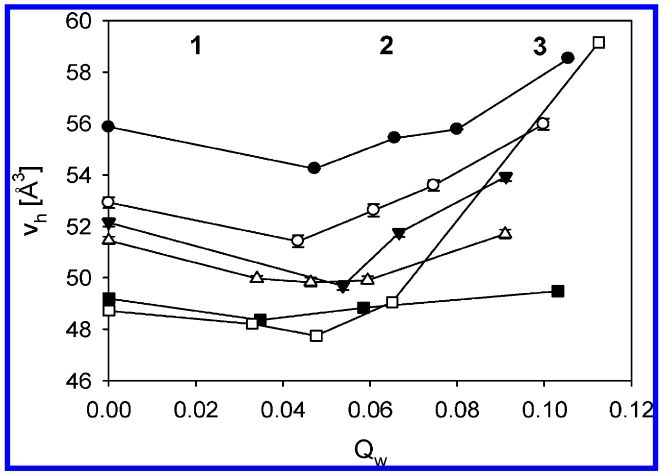

Figure 6. Hole volume measured at 25 °C as a function of water content for matrices of various compositions, equilibrated at a range of water activities between $a_w = 0$ and $a_w = 0.54$ ($T = 25$ °C). Filled circles, $Q'_g = 0$; open circles, $Q'_g = 0.02$; filled triangles, $Q'_g = 0.06$; open triangles, $Q'_g = 0.10$; filled squares, $Q'_g = 0.15$; open squares, $Q'_g = 0.20$. The various regimes discussed in the text are indicated by the numbers 1, 2, and 3, respectively.

molecular packing in the glassy state, therefore, not many rubbery samples were prepared. Unfortunately, this also means that we cannot verify if the hole sizes become independent of the glycerol content for much higher water contents, as was done for maltose in a similar system.[9]

Macroscopic Properties. The sorption of water results in an increase in both the normalized matrix density, ρ/ρ_0, and the matrix expansion, θ, at 25 °C for matrices in the glassy state (Figure 7). Here, the subscript "0" refers to the anhydrous state. Both quantities are nearly independent of the matrix composition, creating what appear to be linear master plots in the water activity range between 0.11 and 0.54. The data series for the normalized density increase and the volumetric swelling as a function of water content can both be fitted well by linear regression. Similar observations have been reported for a

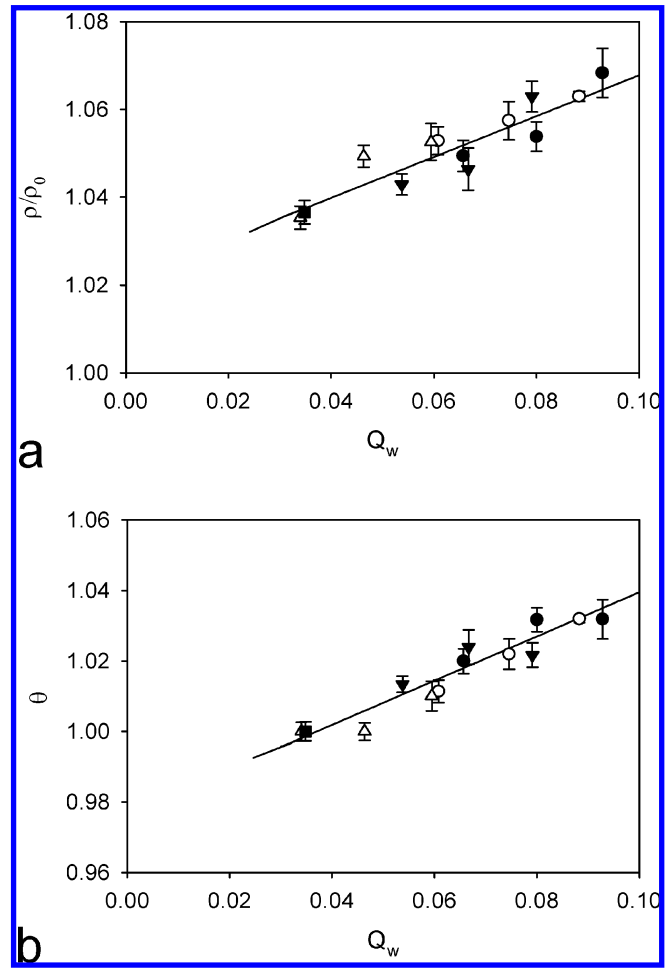

Figure 7. (a) Normalized density increase and (b) degree of matrix swelling, as a function of the water content, Q_w ($T = 25$ °C), for glassy matrices of different glycerol contents. Filled circles, $Q'_g = 0$; open circles, $Q'_g = 0.02$; filled triangles, $Q'_g = 0.06$; open triangles, $Q'_g = 0.10$. The data series for the normalized density increase and the matrix swelling are fitted with linear regression lines with gradients ~0.47 ($R^2 = 0.85$) and ~0.63 ($R^2 = 0.87$), respectively. The dashed lines represent the linear extrapolation of the data to zero water content.

maltopolymer−maltose system.[9] For the maltodextrin−glycerol system, however, we observe nearly double the rate of increase of the normalized density with water content and consequently a less-pronounced matrix swelling compared to the maltopolymer−maltose system. These discrepancies may be explained by the differences in the water vapor sorption of the two systems, illustrated by the converged fitting parameters for the GAB and the Freundlich models (Tables 4 and 5, and Tables 2 and 6 from ref 15).

It is interesting to note that the value of the intercepts of both the normalized density increase (1.02 ± 0.02) and the volumetric expansion (0.98 ± 0.015) deviate from unity. Although this deviation is more or less within the error margin of the fits to the data series, one may be tempted (with appropriate caution) to speculate that this deviation from unity is real in the light of the changes in the size of the molecular free volumes. PALS measurements of matrices with very low water contents ($Q_w < 0.05$) indicate the role of water as an antiplasticizer, whereby it reduces the average hole size in the matrices. In this regime, water molecules are closely associated with the maltodextrin chains without disrupting the hydrogen bonding network. This, together with the fact that water molecules close to carbohydrate chains can pack more efficiently than in bulk water,[4] leads to a

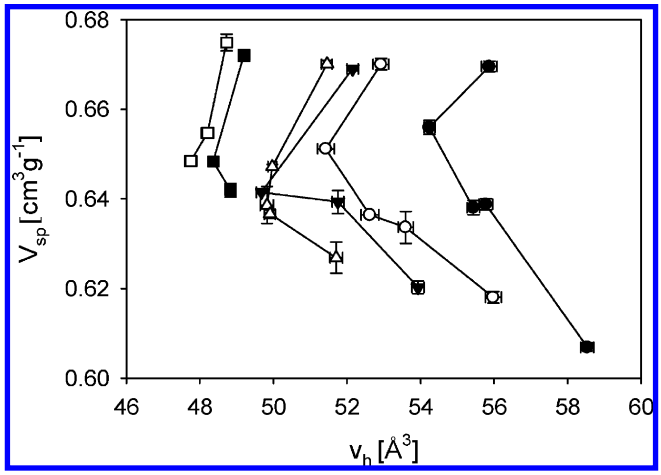

Figure 8. Correlation between hole volume and the specific volume as a function of water content for the various matrix compositions ($T = 25$ °C). Filled circles, $Q'_g = 0$; open circles, $Q'_g = 0.02$; filled triangles, $Q'_g = 0.06$; open triangles, $Q'_g = 0.10$; filled squares, $Q'_g = 0.15$; open squares, $Q'_g = 0.20$.

rapid, nonlinear initial increase in the matrix density. This initial nonlinear behavior for $Q_w < 0.05$ could be invoked to explain the apparent deviation of the intercepts from unity. At slightly higher water contents ($Q_w > 0.05$), while the matrices are still in the glassy state, the normalized density increases linearly as a function of the water content. Unfortunately, there are no measurements in the very low water content region ($Q_w < 0.03$) due to the difficulty in sample equilibration at such low water contents (the diffusion coefficient of water decreases very rapidly with decreasing water content in the glassy state).[52]

Specific Volume - Hole Volume Correlations. The specific volume and the hole volume data for the matrices in the glassy state can be combined to explore the relation between the macroscopic properties and the changes, which occur at the molecular level. The correlation between the specific volume and the hole volume, as a function of water content for different matrix compositions, is shown in Figure 8. A relatively complex relationship emerges, reflecting the role of water both as a plasticizer and as an antiplasticizer.

Deep in the glassy state, at very low water contents, for the matrices with $Q_g > 0.10$, small reductions in hole volume result in significant decreases in the specific volume as the water content increases. This reflects the small initial decrease in the hole volume observed for the matrices with high glycerol weight fraction (denoted as Regime 1 in Figure 6). This positive relationship arises due to the antiplasticizing effect of water at very low water contents, with strong hydrogen-bonding interactions between the carbohydrate chains and water, which leads to a partial hole "filling" and a reduced specific volume with increasing water content.

As the water content increases further, while the matrices are still in the glassy state, there is a negative correlation between the specific volume and the hole volume. An increase in the average molecular hole size is accompanied by a decrease in the specific volume of the matrix. In this regime (corresponding to Regime 2 in Figure 6), the water molecules are still closely associated with the carbohydrate chains (as in Regime 1), principally because the degree of water−carbohydrate hydrogen bonding remains very high. However, the higher water content in Regime 2 increases the local degrees of freedom of the carbohydrate chains, resulting in an increase in the average hole size, while the specific volume still decreases. This complex relation between the specific volume and the hole volume in what may be called the early plasticization regime was also previously reported for water in maltopolymer-maltose matrices.[8] Despite the similarities in behavior however, a clear difference emerges between the two systems. For the maltodextrin−glycerol matrices, we observe a significantly steeper slope of the negative correlation between the specific and the hole volumes than for the maltopolymer−maltose blends studied previously.[8] This results from the greater rate of normalized density increase as a function of water content, which in turn is determined by the differences in the specific molecular properties of glycerol and maltose in the carbohydrate matrices.

Antiplasticization and Plasticization of Maltrodextrin by Glycerol, Water, and Maltose. Figures 5 and 6 demonstrate that in the concentration range studied (0 to 20 wt % on total on anhydrous organic component basis), glycerol reduces the average hole size in the glassy state. Following the free-volume interpretation, glycerol therefore has an antiplasticizing effect on the maltodextrin matrices in this regime. By using the argument set out above for water, it can be calculated that the observed reduction in hole volume caused by glycerol cannot be accounted for by a simple "hole filling". The observed reduction in hole size is about fifteen times smaller than what is expected from a simple "hole filling" mechanism. It is clear, therefore, that instead the reduction in the average molecular hole size results from changes in molecular packing due to composition-related differences in the dependence of the matrix dynamics on water content and temperature. The chains of the maltodextrin matrices are strongly entangled due to their relatively high molecular weight. Glycerol, due to its small size causes a reduction in the density of these entanglements and is also likely to interfere with the hydrogen bonding between the maltodextrin chains. Some of the carbohydrate−carbohydrate hydrogen bonds may be replaced by carbohydrate−glycerol hydrogen bonds. In a mechanism that bears some similarity to the plasticization by water, glycerol is likely to disrupt the carbohydrate−carbohydrate hydrogen bonds, facilitating the rearrangements of the carbohydrate chains and, hence, altering the structure of the matrix. The effect glycerol has on the molecular packing of the maltodextrin matrices may be compared to this of other small molecules, such as water and maltose.

Owing to its smaller molecular size and the different balance between proton donors and acceptors, water alters the molecular packing of the matrices in a somewhat different way compared to glycerol. This results in an antiplasticizing regime for a significantly smaller range of water contents (Figure 6, refs 8 and 9). The antiplasticization regime for water, as determined from PALS measurements on maltodextrin−glycerol matrices, agrees very well with the predictions from the equation-of-state analysis for thermoplastic starch, which is based on PVT measurements.[10] In our studies, we have limited the glycerol concentration in the matrices to a maximum of 20 wt %, but based on the behavior of water in the matrices, we infer that at higher glycerol concentrations, the hole size may pass through a minimum before it starts to increase.

The effect of maltose on the molecular organization of maltopolymer glasses bears a striking similarity to the effect of glycerol on the maltodextrin matrices.[8,9] For maltopolymer−maltose glasses, the antiplasticization regime extends over the full maltose concentration range from 0 to 100 wt % on total carbohydrate at $T = 25$ °C. The antiplasticization regime for maltose in such carbohydrate glasses is, thus, much larger than what observed for water and is also likely to be larger than for glycerol. As observed for both glycerol and water, the

decrease in hole size as a function of maltose weight fraction is most likely accounted for by changes in matrix dynamics resulting from the addition of maltose, rather than on a hole filling mechanism. In summary, we infer from our studies that the antiplasticizing and plasticizing behavior of diluents in glassy carbohydrate matrices depends in a sensitive manner on a balance between the molecular size and the interactions of the diluent molecules with the carbohydrate chains.

Concluding Remarks

We have systematically explored the effect of glycerol, a low molecular weight polyol, on the molecular packing of maltodextrin matrices by Positron Annihilation Lifetime Spectroscopy. The effect of this low molecular weight polyol on the molecular organization of these matrices was also compared to the effects of two other small molecules: water and maltose. The PALS measurements at the nanolevel were combined with thermodynamic measurements and dilatometry to illustrate the role of glycerol as a packing enhancer in the glassy state. Provided the matrices are in the glassy state, we observe a systematic reduction in the average molecular hole size of the amorphous matrix. The effect of glycerol as an antiplasticizer closely mimics the behavior of maltose in maltopolymer matrices but for a more limited range of concentrations. The impact of water on the local molecular organization of glassy carbohydrates is more complex than that of either glycerol or maltose. At very low water contents, it acts as an antiplasticizer, whereby it reduces the average molecular hole size. However, at slightly higher water contents, while the matrices are still in the glassy state, water acts as a plasticizer, whereby increasing the average hole size. The results on the molecular packing in maltodextrin−glycerol matrices presented here are of importance, because they provide a first indication of how the molecular structure and packing of such matrices could relate to the fast dynamic modes in carbohydrate−glycerol matrices. It is likely that because of the more densely packed structure in the presence of glycerol, several relevant dynamic modes are suppressed, leading to an improved the encapsulation and biostabilization performance of glassy carbohydrate matrices containing limited fractions of glycerol.[13] In this sense, glycerol affects the molecular packing of the carbohydrate matrices in a similar way to disaccharides, such as maltose.[9] Based on our results, we expect that the concentration range in which glycerol is an effective packing enhancer is significantly smaller than for maltose.

References and Notes

(1) Langer, M.; Holtje, M.; Urbanetz, N. A.; Brandt, B.; Holtje, H. D.; Lippold, B. C. *Int. J. Pharm.* **2003**, *252*, 167–179.
(2) Levine, H. *Amorphous Food and Pharmaceutical Systems*; Royal Society of Chemistry: London, 2002.
(3) Crowe, J. H.; Oliver, A. E.; Hoekstra, F. A.; Crowe, L. M. *Cryobiology* **2004**, *35*, 20–30.
(4) Kilburn, D.; Claude, J.; Schweizer, T.; Alam, A.; Ubbink, J. *Biomacromolecules* **2005**, *6*, 864–879.
(5) Cicerone, M. T.; Tellington, A.; Trost, L.; Sokolov, A. *Bioprocess Int.* **2003**, *1*, 36–47.
(6) Ubbink, J.; Kasapis, S.; Norton, I. T.; Ubbink, J. *Modern Biopolymer Science*; Academic Press: New York, 2009; pp 277−293.
(7) Kilburn, D.; Claude, J.; Mezzenga, R.; Dlubeck, G.; Alam, A.; Ubbink, J. *J. Phys. Chem. B* **2004**, *108*, 12436–12441.
(8) Townrow, S.; Kilburn, D.; Alam, A.; Ubbink, J. *J. Phys. Chem. B* **2007**, *111*, 12643–12648.
(9) Townrow, S.; Roussenova, M.; Giardiello, M.; Alam, A.; Ubbink, J. *J. Phys. Chem. B* **2010**, *114*, 1568–1578.
(10) Benczédi, D.; Tomka, I.; Esher, F. *Macromolecules* **1998**, *31*, 3062–3074.
(11) Derbyshire, W.; Van den Bosch, M.; Dusschoten, D.; Mac Naughton, W.; Farhat, I.; Hemminga, M. A.; Mitchell, J. R. *J. Magn. Reson.* **2004**, *168*, 278–283.
(12) Roudaut, G.; Farhat, I.; Poirier-Brulez, F. D. *Carbohydr. Polym.* **2009**, *77*, 489–495.
(13) Cicerone, M. T.; Soles, C. L. *Biophys. J.* **2004**, *86*, 3836–3845.
(14) van den Dries, I. J.; van Dusschoten, D.; Hemminga, M. A. *J. Phys. Chem. B* **1998**, *102*, 10483–10489.
(15) van den Dries, I. J.; van Dusschoten, D.; Hemminga, M. A.; van der Linden, E. *J. Phys. Chem. B* **2000**, *104*, 10126–10132.
(16) Noel, T. R.; Parker, R.; Ring, S. R. *Carbohydr. Res.* **2000**, *329*, 839–845.
(17) Anandamaran, S.; Reineccius, G. A. *Food Technol.* **1986**, *40*, 88−93.
(18) Lourdin, D.; Bizot, H.; Colonna, P. *J. Appl. Polym. Sci.* **1996**, *63*, 1047–1053.
(19) Anopchenko, A.; Psurek, T.; VanderHart, D.; Douglas, J. F.; Obrzut, J. *Phys. Rev. E* **2006**, *74*, 031501–031510.
(20) Maeda, Y.; Paul, D. R. *J. Polym. Sci., Part B* **1987**, *25*, 981–1003.
(21) Benczédi, D.; Tomka, I.; Escher, F. *Macromolecules* **1998**, *31*, 3055–3061.
(22) Maeda, Y.; Paul, D. R. *J. Polym. Sci., Part B* **1987**, *25*, 957–980.
(23) You, Y.; Ludescher, R. D. *Food Biophys.* **2007**, *2*, 133–145.
(24) Roussenova, M.; Andrieux, J.-C.; Alam, A.; Ubbink, J. Manuscript in preparation.
(25) Bell, L. N.; Labuza, T. P. *Moisture Sorption: Practical Aspects of Isotherm Measurement and Use*, 2nd ed.; American Association of Cereal Chemists: St. Paul, MN, 2000.
(26) Ubbink, J.; Giardiello, M.; Limbach, H. J. *Biomacromolecules* **2007**, *8*, 2862–2873.
(27) Flory, P. *J. Chem. Phys.* **1942**, *10*, 51–61.
(28) Adamson, A. W. *Physical Chemistry of Surfaces*, 2nd ed.; Interscience: New York, 1967.
(29) Brunauer, S.; Emmett, P. H.; Teller, E. *J. Am. Chem. Soc.* **1938**, *60*, 309–319.
(30) Anderson, R. B. *J. Am. Chem. Soc.* **1946**, *68*, 686–691.
(31) Zimm, B. H.; Lundberg, J. L. *J. Phys. Chem.* **1956**, *60*, 425–428.
(32) Kirkwood, J. G.; Oppenheim, I. *Chemical Thermodynamics*; Blaisdell: New York, 1964.
(33) Hill, T. L. *Statistical Mechanics*; McGraw-Hill: New York, 1961.
(34) Roos, Y. H. *Phase Transitions of Foods*; Academic Press: San Diego, CA, 1995.
(35) Chronakis, I. S. *Crit. Rev. Food. Sci.* **1998**, *38*, 599–637.
(36) Greenspan, L. *Res. Natl. Bur. Stand.* **1977**, *81A*, 89–96.
(37) Jean, Y. C.; Mallon, P. E.; Schrader, D. M. *Positron and Positronium Chemistry*; World Scientific: River Edge, NJ, 2003.
(38) Pethrick, R. A. *Prog. Polym. Sci.* **1997**, *22*, 1–47.
(39) Tao, T. J. *J. Chem. Phys.* **1972**, *56*, 5499–5510.
(40) Eldrup, M.; Lightbody, D.; Sherwood, J. N. *Chem. Phys.* **1981**, *63*, 51–58.
(41) Kansy, J. *Nucl. Instrum. Methods* **1996**, *374*, 235–244.
(42) Kansy, J. *LT for Windows*, version 9.1, PL-40-007 Katowice; Institute of Physical Chemistry of Metals: Silesian University, Bankowa 12, Poland, October 2008; private communication.
(43) Gordon, M.; Taylor, J. S. *J. Appl. Chem.* **1952**, *2*, 493–500.
(44) Slade, L.; Levine, H. *Adv. Food Nutr. Res.* **1995**, *38*, 103–269.
(45) Franks, F. *Water: Matrix of Life*, 2nd ed.; Royal Society of Chemistry: Cambridge, U.K., 2000.
(46) Roos, Y.; Karel, M. *J. Food Sci.* **1991**, *56*, 1676–1681.
(47) Roos, Y. *Carbohydr. Res.* **1993**, *238*, 39–48.
(48) Lourdin, D.; Colonna, P.; Ring, S. G. *Carbohydr. Res.* **2003**, *338*, 2883–2887.
(49) Surana, R.; Pyne, A.; Suryanarayanan, R. *Pharm. Res.* **2004**, *21*, 867–874.
(50) Enrione, J.; Hill, S. E.; Mitchell, J. R. *J. Agric. Food Chem.* **2007**, *55*, 2956–2963.
(51) Limbach, H. J.; Ubbink, J. *Soft Matter* **2008**, *4*, 1887–1898.
(52) Tromp, R. H.; Parker, R.; Ring, S. G. *Carbohydr. Res.* **1997**, *303*, 199–205.
(53) Yamamoto, R.; Onuki, A. *Phys. Rev. Lett.* **1998**, *81*, 4915–4918.

BM1005068